

Beat-to-beat Adaptation of QT Interval to Heart Rate

Esther Pueyo, Marek Malik and Pablo Laguna

Abstract—An adaptive approach is presented to investigate the QT interval response to heart rate variations on a beat-to-beat basis. The relationship between the QT interval and the RR interval is modelled by considering a time-variant system composed of a linear filter followed by a zero-memory nonlinearity approximated by a Taylor expansion. The linear portion describes the influence of previous RR intervals on each QT measurement, while the nonlinear portion expresses how the QT values evolve as a function of the averaged RR measurement at the output of the linear filter. For identification of the unknown system, a Kalman-based procedure is developed that simultaneously estimates all the parameters of the global system. The methodology has been first tested over artificially generated data, showing very good agreement between estimated and theoretical values. Results on data measured over real ECG recordings confirm that the QT interval response is delayed with respect to the RR interval, specially for decelerating heart rate changes. It is also shown that the beat-to-beat evolution of the nonlinearity coefficients is considerably altered when abrupt rate variations occur.

I. INTRODUCTION

THE QT interval, expressing overall duration of ventricular repolarization, has been one of the most studied indexes of the surface electrocardiogram (ECG), since it has been extensively reported that impaired adaptation of the ventricular repolarization time to changes in heart rate may be associated with the risk of cardiac arrhythmias [1]. Many of the studies that analyze the relationship between QT and RR (inverse of heart rate) are restricted to episodes where the RR signal is stable [2], over which it is generally accepted that QT is mainly influenced by the immediately preceding RR interval. In [3] a method was proposed to assess QT interval dynamics in response to RR changes on ambulatory recordings and characteristics of the adaptation in terms of both duration and profile were individually provided for each recording and also for selected segments presenting abrupt RR changes. However, with such a method it is not possible to evaluate the QT dynamic behaviour on a beat-to-beat basis, which might be very useful for the determination of instants where disturbances in the adaptation occur. In this study, we provide a full beat-to-beat adaptation analysis that

This work was supported by project TEC2004-05263-C02-02/TCM from MCYT/FEDER

E. Pueyo is with the Communications Technology Group (GTC) at the Aragón Institute for Engineering Research (I3A), University of Zaragoza, 50018 Zaragoza, Spain epueyo@unizar.es

M. Malik is with the Department of Cardiological Sciences, St. George's Hospital Medical School, SW17 ORE London, United Kingdom m.malik@sghms.ac.uk

P. Laguna is with the Communications Technology Group (GTC) at the Aragón Institute for Engineering Research (I3A), University of Zaragoza, 50018 Zaragoza, Spain laguna@unizar.es

can describe changes in the QT interval and relate them with the variations in heart rate.

To perform the investigation, we propose the consideration of a general model that when applied to ECG data takes the RR series as the input signal x and the QT series as the output signal y . The proposed model allows for nonlinear and time-varying input-output relations and, moreover, the input signal x is considered to be possibly nonstationary. These facts make the adaptive filter proposed for parameter estimation operate in a nonstationary environment. To deal with that, we propose a procedure for identification of the unknown system based on the Kalman filter [4], [5], which can be seen as a sequential minimum mean-square error estimator when the system varies in time according to a dynamical state-space model [5].

The described methodology has been first evaluated using simulated data and subsequently applied to the analysis of real ECG recordings.

II. METHODS

A. Model composition

We use a nonlinear system with memory to model the relationship between scalar and real input and output signals, $x(n)$ and $y(n)$. The input signal $x(n)$ is the realization of a stochastic process that may be nonstationary and for which no a priori probability density function (pdf) distribution is assumed. In the application to ECG data $x(n)$ will be represented by the RR series. The system to be identified, represented in figure II-A, is assumed to be composed of a linear FIR time-variant filter of order N :

$$\mathbf{h}(n) = [h_0(n), \dots, h_{N-1}(n)]^T \in \mathbb{R}^{N \times 1},$$

followed by a time-varying zero-memory non-linearity g expandable as a P -th order Taylor series around a bias point:

$$g(z(n), \mathbf{a}(n)) = \sum_{k=0}^P a_k(n) z(n)^k,$$

with $\mathbf{a}(n) = [a_0(n), \dots, a_P(n)]^T \in \mathbb{R}^{(P+1) \times 1}$. The orders N and P are defined a priori based on the characteristics of the input and output signals to be processed. An additional restriction is imposed on the linear filter to guarantee uniqueness in the estimation of the filter weights and the nonlinearity coefficients: $\mathbf{h}(n)^T \mathbf{1} = 1, \forall n$, with $\mathbf{1}$ denoting the N -length column vector of ones. With such a restriction, the output of the linear portion, $z(n) = \mathbf{h}(n)^T \mathbf{x}(n)$, with

$$\mathbf{x}(n) = [x(n), x(n-1), \dots, x(n-N+1)]^T,$$

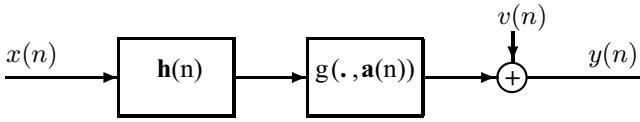


Fig. 1. Block structure of the system considered in the study composed of a linear FIR time-variant filter $\mathbf{h}(n)$ followed by a time-varying nonlinear function $g(\cdot, \mathbf{a}(n))$. The output of the system is corrupted by independent additive noise $v(n)$.

can be interpreted in the *ECG* application as a weighted-averaged *RR* measurement with weights specifically defined at each instant n . The nonlinear subsystem is representative of how the *QT* interval (output signal) evolves as a function of the averaged *RR* measurement.

The output of the unknown system is assumed to be corrupted by additive white noise $v(n)$ uncorrelated with the input $x(n)$. The noise signal $v(n)$ can include, for instance, delineation errors generated in the determination of the *QT* interval. Thus, the output of the global system can be written as

$$y(n) = g(z(n), \mathbf{a}(n)) + v(n) = \mathbf{a}(n)^T \mathbf{z}(n) + v(n),$$

where $\mathbf{z}(n) = [1, z(n), \dots, z(n)^{P-1}]^T$, $z(n) = \mathbf{h}(n)^T \mathbf{x}(n)$.

B. Adaptive estimation of model parameters

The Taylor series expansion approximating the nonlinear function is first converted into a relation that allows to express the output of the unknown system as a linear combination of functions of the input signal, as explained in section II-B.1. Then, a linear adaptive filter is used to estimate the coefficients of such a combination following the approach described in sections II-B.2 and II-B.3.

1) *Volterra series expansion*: In section II-A we described the model structure considered in this study, which corresponds to a time-variant polynomial system whose output $y(n)$ is expressed in terms of its input $x(n)$ by the relation

$$y(n) = \sum_{k=0}^P a_k(n) \left(\sum_{i=0}^{N-1} h_i(n) x(n-i) \right)^k,$$

and such an output is subsequently corrupted by some additive white noise $v(n)$. Denoting $m_0(n) = a_0(n)$ and

$$m_k(i_1, i_2, \dots, i_k; n) = \frac{k!}{\prod_{t=0}^{N-1} l_t!} a_k(n) \prod_{j=1}^k h_{i_j}(n),$$

where l_t counts the number of indexes in $\{i_1, i_2, \dots, i_k\}$ that are equal to t , the above expression for $y(n)$ can be transformed into a new one having the property of being linear in its parameters, as shown in (1).

Moreover, by introducing the notation

$$\mathbf{m}(n) = [\mathbf{m}^0(n)^T, \mathbf{m}^1(n)^T, \dots, \mathbf{m}^P(n)^T]^T,$$

where $\mathbf{m}^k(n) = [m_k(0, \dots, 0, 0; n), m_k(0, \dots, 0, 1; n), \dots, m_k(N-1, \dots, N-1; n)]^T$, $1 \leq k \leq P$, and

$$\mathbf{s}(n) = [\mathbf{s}_0(n)^T, \mathbf{s}_1(n)^T, \dots, \mathbf{s}_P(n)^T]^T,$$

with $\mathbf{s}_0(n) = 1$ and $\mathbf{s}_k(n) = [x(n)^k, x(n)^{k-1}x(n-1), \dots, x(n-N+1)^k]^T$, $1 \leq k \leq P$, the output of the global system, after incorporation of the noise $v(n)$, can be expressed in vector form as

$$y(n) = \mathbf{s}(n)^T \mathbf{m}(n) + v(n),$$

with $\mathbf{s}(n)$ being the known observation vector and $\mathbf{m}(n)$ being the parameter vector to be estimated.

2) *State-space formulation*: The underlying model, in the form described in section II-B.1 after application of the linearization procedure, is now formulated in terms of a state-space representation (see[4], pp. 470).

The finite-dimensional linear state-space model for the output process $y(n)$ is defined by a pair of equations: a *measurement equation*, which expresses $y(n)$ as

$$y(n) = \mathbf{s}(n)^T \mathbf{m}(n) + v(n), \quad n \geq 0,$$

where $\mathbf{m}(n)$ is called the *state-vector*; and a *process equation*, which describes the recursion that obeys the state-vector as

$$\mathbf{m}(n+1) = \mathbf{F}(n)\mathbf{m}(n) + \mathbf{u}(n), \quad n \geq 0.$$

being $\mathbf{F}(n)$ called *transition matrix*. The processes $v(n)$ and $\mathbf{u}(n)$, termed *measurement noise* and *process noise*, respectively, are assumed to be zero-mean white noise processes. Unless there is feedback from the output to the states, such noises can be assumed to be uncorrelated, as it is the case for our purposes. The initial state $\mathbf{m}(0)$ is assumed to be a zero-mean random vector with covariance matrix $\mathbf{\Pi}_0$ and uncorrelated with $v(n)$ and $\mathbf{u}(n)$. In our implementation of the Kalman filter, the state estimate at time $n=0$ is assigned a value equal to zero and the matrix $\mathbf{\Pi}_0$ is taken as the identity matrix. The assumptions on the model can be written as

$$E \left\{ \begin{pmatrix} \mathbf{u}(n) \\ v(n) \\ \mathbf{m}(0) \\ 1 \end{pmatrix} \begin{pmatrix} \mathbf{u}(n) \\ v(n) \\ \mathbf{m}(0) \end{pmatrix}^T \right\} = \begin{pmatrix} \mathbf{Q}(n)\delta_{nm} & 0 & 0 \\ 0 & \mathbf{R}(n)\delta_{nm} & 0 \\ 0 & 0 & \mathbf{\Pi}_0 \\ 0 & 0 & 0 \end{pmatrix}.$$

where $\mathbf{Q}(n)$ is the covariance matrix of the process noise and $\mathbf{R}(n)$ is the variance of the measurement noise. In addition, in the application of the Kalman filter it is assumed that the matrices $\mathbf{F}(n), \mathbf{s}(n), \mathbf{Q}(n), \mathbf{R}(n)$ and $\mathbf{\Pi}_0$ are known a priori. For our problem, the matrices $\mathbf{F}(n), \mathbf{Q}(n)$ and $\mathbf{R}(n)$ are not known and need to be estimated from samples of the input and output signals. This is done following the methodology developed in the next subsection.

Once the linear state-space model has been formulated, the Kalman filter is applied to optimally solve the process and measurement equations for the unknown state vector $\mathbf{m}(n)$, which can be thought of as the minimal set of data sufficient to describe the system behaviour [4].

3) *Estimation of the transition matrix and the noises' covariances*: Matrices $\mathbf{F}(n), \mathbf{Q}(n)$ and $\mathbf{R}(n)$ are estimated by extending the method proposed in [6] to deal with the more general case of those matrices being time-variant and the input process having a nonstationary behaviour. In

$$y(n) = m_0(n) + \sum_{k=1}^P \sum_{i_1=0}^{N-1} \sum_{i_2=i_1}^{N-1} \dots \sum_{i_k=i_{k-1}}^{N-1} m_k(i_1, i_2, \dots, i_k; n) \prod_{j=1}^k x(n - i_j) \quad (1)$$

[6], the technique developed for estimating \mathbf{F} , \mathbf{Q} and \mathbf{R} does not make any a priori assumption about the system dynamics, but, on the contrary, uses only the information contained in the stationary observation vector $\mathbf{x}(n)$ and the nonstationary output signal $y(n)$. Such information is utilized to compute the average autocorrelations of the processes $y(n)$ and $\mathbf{b}(n) = y(n)\mathbf{x}(n)$ as well as higher order standard moments of the stationary input vector $\mathbf{x}(n)$. These quantities are used to determine the average autocorrelation $\mathbf{C}_w(m)$ of the unknown system response $\mathbf{w}(n)$ and the autocorrelation $c_v(m)$ of the additive noise $v(n)$ for different values of lag m , by solving a system of linear equations. With the values obtained for $\mathbf{C}_w(m)$ and $c_v(n)$, a straightforward method is provided to deduce \mathbf{F} , \mathbf{Q} and \mathbf{R} .

In our study, a different system of linear equations is set up for each time instant n , where the known quantities involved in the equations are now estimates of the autocorrelations for the nonstationary processes $y(n)$, $\mathbf{s}(n)$ and $\mathbf{b}(n) = y(n)\mathbf{s}(n)$, evaluated at times n and $n + m$, for different values of lag m . For computation of those autocorrelations we used the procedure proposed in [7], which is based on the evolutionary spectral theory. The subsequent steps followed to obtain estimates of $\mathbf{F}(n)$, $\mathbf{Q}(n)$ and $\mathbf{R}(n)$ are analogous to the ones described in [6], but now separately applied at each time instant n .

III. DATA

A. Population

The study evaluated ECG recordings obtained from 38 healthy subjects during controlled postural manoeuvring. Continuous 12-lead electrocardiograms were recorded while subjects were changing their postural position from supine to sitting, from sitting to standing, ..., which resulted in substantial and frequently very abrupt changes in heart rate. This type of recordings provided us with a very useful tool for analysing the mode of adaptation of the QT interval to both accelerations and decelerations in heart rate.

B. Data measurement

For each ECG recording, the lead presenting the greatest signal-to-noise ratio was identified. On such a lead, RR and QT intervals were measured using the automatic wavelet transform-based delineation system described in [8]. The obtained RR and QT series were reviewed to avoid potential outliers. Subsequently, the series were linearly interpolated at sampling frequency of 1 Hz. We then enlarged them by repetition so that, after processing by our proposed algorithm, we could discard the first half and thus avoid the initial estimation values that corresponded to the transient mode of the algorithm.

IV. RESULTS

A. Simulation results

In order to assess the performance of the adaptive procedure proposed in this study, we performed two different kinds

of simulations. In both types of simulations, we considered a real RR series as the input signal. We then fixed the values of the system parameters to be identified and generated the corresponding output signal. Such input and output signals constituted all the information provided to the algorithm, which tried to estimate the actual parameter values.

For the first kind of simulations, the system parameters (i.e. the weights of the linear filter and the coefficients of the nonlinearity) were considered to be time-invariant. As an example, we describe the results obtained when we selected a third order linear filter with impulse response $\mathbf{h}(n) = [0.5, 0.3, 0.2]^T$, and a first-order Taylor polynomial with coefficients $\mathbf{a}(n) = [0.3, 0.045]^T$. The output of the global system was subsequently corrupted by additive white gaussian noise with an SNR of 20 dB. For the simulation, the orders of the filter and the nonlinear function were not known a priori and were set to 5 and 1, respectively. The algorithm identified that the order of the actual linear filter was three and gave the fourth and fifth weights values very close to zero, while the converged estimated values for the first three weights were in very close agreement with the actual ones. The converged coefficients of the nonlinearity successfully approximated the theoretical ones as well. A measure of the algorithm's performance was provided by the relative mean-square deviation, defined as the ratio between the squared norm of the parameter-error vector and the squared norm of the actual parameter vector. Such a measure was below 10^{-10} at all time instants.

For the second kind of simulations, the system parameters were selected as time-varying. Three filter weights were generated from sinusoidal functions that produced slowly varying evolutions, while a first-order nonlinearity coefficient vector was chosen containing components with sinusoidal and linear functions, respectively. The good agreement between theory and simulations was corroborated as well. The relative mean-squared deviation was in this case always below 10^{-7} . We can conclude that our algorithm was able to track the temporal variations of both the linear filter and the nonlinear function.

B. ECG analysis

The methodology developed in our study was applied to investigate the mode of adaptation of the QT interval to changes in heart rate. The most important contribution of our method to the analysis of the repolarization adaptation is that it provides a tool for studying how the relationship between QT and RR evolves with time on a beat-to-beat basis. From a physiological point of view, it is reasonable to expect that QT dependence on heart rate can have different characteristics according to whether the recording segment being analysed corresponds to a period where heart rate is stable or, on the contrary, it presents abrupt variations. As an example, figure 2 contains the RR and QT interval series corresponding to one of the recordings analysed in the study

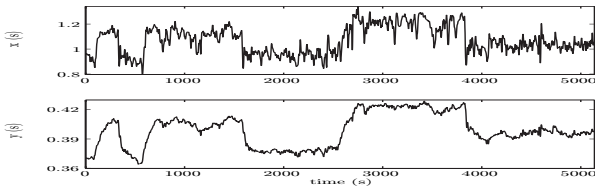


Fig. 2. RR and QT interval series for one of the body postural recordings analysed in the study.

and figure 3 shows the beat-to-beat evolution of the linear filter weights. It can be seen that the first weight, which expresses the QT dependence on the immediately preceding RR interval, tends to decrease when a sudden and marked change in rate occurs. This fact enforces the idea that it is necessary to account for the influence of previous RR intervals, rather than just the preceding one, when analysing the QT/RR relationship. Also, it can be observed that the lag in the adaptation is much more pronounced when heart rate decelerates (i.e. RR increases) than when it accelerates. Even though the graphic is presented only for the case of three filter weights, results have been derived for much longer filter lengths in order to evaluate the QT lag in a more meaningful way, thus being able to identify, on a beat-to-beat basis, those RR intervals that effectively contribute to QT variations. In figure 4, the evolution of the nonlinearity coefficients is presented for the same recording shown in figure 2. A first-order Taylor polynomial has been considered for the plot in order to be able to interpret the results in terms of slope and ordinate, even results were also derived using higher-order nonlinear functions. It can be noticed that both the slope and the ordinate considerably change in abrupt rate transitions.

A piece of the same recording containing a very abrupt change in rate has been selected and plotted in figure 5 (left panel), where segments corresponding to decelerating, stable and accelerating heart rate have been independently analysed. Again, it is clear from the graphic that QT adapts to an accelerating change in rate much faster than it does for a decelerating one. When heart rate stabilizes to a certain level, the nonlinearity coefficients also oscillate around a definite value. As a final point, we show in figure 5 (right panel) a hysteresis plot associated with this same piece of recording. Such a hysteresis plot was created by representing the nonlinearity g in a neighbourhood of each RR -averaged measurement obtained at the output of the linear system. It is clearly noticeable that for the same range of RR values considered both for the accelerating and decelerating periods, the ranges of QT values are substantially different, which confirms that QT cannot be determined only as a function of its preceding RR interval, but, on the contrary, it strongly depends on a past history of RR intervals.

V. CONCLUSIONS

The proposed methodology allows to describe the QT/RR relationship in a dynamic way. It remains to evaluate the diagnostic value for arrhythmic risk prediction of the information provided by the described approach.

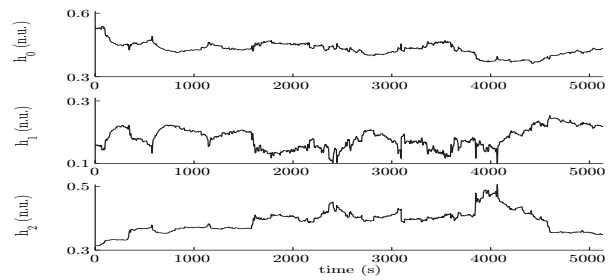


Fig. 3. Temporal evolution of the linear filter weights corresponding to the series presented in figure 2.

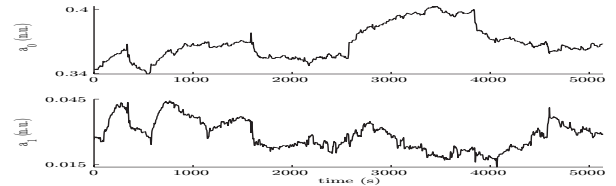


Fig. 4. Temporal evolution of the nonlinearity coefficients corresponding to the series presented in figure 2.

REFERENCES

- [1] A. Pathak, D. Curnier, J. Fourcade, J. Roncalli, P. K. Stein, P. Hermant, M. Bousquet, P. Massabuau, J. M. Senard, J. L. Montastruc, and M. Galinier, "QT dynamicity: a prognostic factor for sudden cardiac death in chronic heart failure," *Eur J Heart Fail*, vol. 7(2), pp. 269–275, Mar. 2005.
- [2] F. Badilini, P. Maison-Blanche, R. Childers, and P. Coumel, "QT interval analysis on ambulatory electrocardiogram recordings: a selective beat averaging approach," *Med Biol Eng Comput*, vol. 37, pp. 71–79, Jan. 1999.
- [3] E. Pueyo, P. Smetana, P. Caminal, A. B. de Luna, M. Malik, and P. Laguna, "Characterization of QT interval adaptation to RR interval changes and its use as a risk-stratifier of arrhythmic mortality in amiodarone-treated survivors of acute myocardial infarction," *IEEE Trans Biomed Eng*, vol. 51(9), pp. 1511–1520, Sept. 2004.
- [4] S. Haykin, *Adaptive filter theory*. Upper Saddle River, NJ: Prentice Hall, 2002.
- [5] S. M. Kay, *Fundamentals of statistical signal processing: Estimation theory*. Englewood Cliffs, NJ: Prentice Hall, 1993.
- [6] Y. Yang and H. Lev-Ari, "Identification of linear time-variant systems without using prior information," in *Proc. IEEE Conf on Acoustics, Speech and Signal Processing*, 2002, pp. 1741–1744.
- [7] A. S. Kayhan, A. El-Jaroudi, and L. F. Chaparro, "Data-adaptive evolutionary spectral estimation," *IEEE Trans Signal Processing*, vol. 43(1), pp. 204–213, Jan. 1995.
- [8] J. Martinez, R. Almeida, S. Olmos, A. Rocha, and P. Laguna, "A Wavelet-Based ECG Delineator: Evaluation on Standard Databases," *IEEE Trans Biomed Eng*, vol. 51(4), pp. 570–581, Apr. 2004.

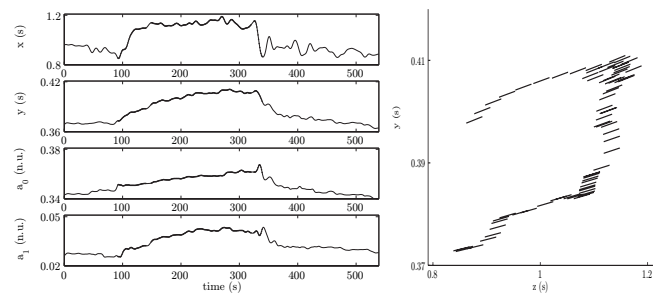


Fig. 5. In the left panel, the RR and QT interval series and estimated coefficients of the nonlinear function corresponding to a selected segment presenting a marked heart rate change are presented. In the right panel, the effect of the hysteresis phenomenon is shown by representing the nonlinearity in a neighbourhood of each time instant of the same episode.